PSFC/JA-08-3

Effects of energy loss on interaction dynamics of energetic electrons with plasmas

C. K. Li and R. D. Petrasso

1 November 2008

Plasma Science and Fusion Center
Massachusetts Institute of Technology
Cambridge, MA 02139 USA

Effects of energy loss on interaction dynamics of energetic electrons with plasmas

C. K. Li and R. D. Petrasso

Plasma Science and Fusion Center, Massachusetts Institute of Technology, Cambridge, Massachusetts 02139, USA

An analytic model is developed for energetic electrons interacting with plasmas. This model rigorously treats the effects of energy loss upon the Coulomb interactions and reveals several new and important features never before unrealized, including the inextricable coupling of scattering and energy loss which previous calculations erroneously treated as independent. The unique transparency and generality of these calculations allows for straightforward applications in the cases of partial and even total energy loss of energetic electrons: for example, the quantitative evaluation of energy deposition of the energetic electrons in various plasmas, including inertial confinement fusion plasmas.

The interaction of energetic electrons with plasmas is a fundamental problem with important implications for both basic physics and practical applications [1-6]. Such an interaction involves electron energy loss and scattering, leading to electron energy deposition and trajectory bending in the plasmas. In the context of a single electron interacting with plasmas, for example, such scatterings stochastically cause electron spatial distributions, consequently resulting in modifications of the detailed energy deposition structure [7-9].

In addressing electron scattering in plasmas, the conventional assumption has been that energetic electrons scatter off plasma ions while losing their kinetic energy to the plasma electrons. Because of the significant mass difference between electrons and background ions, the energy loss to the ions has been neglected. In addition, the two physics processes (*i.e.* energy loss and scattering) have been treated independently and subsequently combined in a simple way. For example, the mean-square of the deflection angle has been calculated simply by averaging over the solid angle

$$\langle \theta^2 \rangle = \frac{N_c \int \theta^2 \left(\frac{d\sigma}{d\Omega} \right) d\Omega}{\int \left(\frac{d\sigma}{d\Omega} \right) d\Omega} \quad , \qquad (1)$$

where N_c = is the number of the collisions (which is a function of the electron energy loss and can be independently evaluated) [10]. The treatment of the scattering is exclusively manifested by the integral $\int \theta^2 (d\sigma/d\Omega) d\Omega$. It has been demonstrated that this approach is justified and is accurate for energetic electrons interacting with thin solid foil [11] since an electron suffers only a relatively small number of collisions ($\sim 10^2$-10^3), and the energy loss of each individual collision is very small compared to its total kinetic energy due to the nature of small-angle dominant Coulomb interactions. Because of this, the energy-dependence in the

scattering cross sections can be essentially overlooked. The same is true for high Z plasmas because *e-ion* scattering so dominates ($\propto Z^2$, and $Z > 1$ for any metal foils) over *e-e* scattering [7-9].

However, such a "thin" approximation is unjustified and inaccurate when it is applied in the case where (for example, during plasma heating) an electron loses a significant amount or all of its energy and suffers a very large number (over $\sim 10^6$ collisions), or when an electron interacts with hydrogenic sittings ($Z=1$, for which the *e-e* scattering could be comparable with the *e-ion* scattering). An example of this is elucidated by Fig. 1 where *e-ion* (Rutherford) and *e-e* (Møller) scattering cross sections are plotted as a function of the energy loss [$\Delta E=(E_0-E)/E_0$] for 1-MeV electrons in hydrogenic sittings. When ΔE changes from beginning to end ($0 \rightarrow 100\%$ of the energy loss), these cross sections increase over 4 order of magnitudes, indicating that the effects of energy loss on scattering can not be ignored, and that a rigorous approach to the inextricable coupling of the energy loss to scattering is necessary.
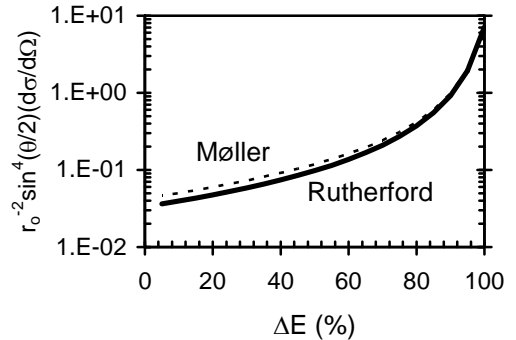

FIG. 1. The normalized Rutherford cross section (*e-ion* scattering) and Møller cross section (*e-e* scattering) are plotted as a function of the fraction of the energy loss for 1-MeV electrons. Both cross sections show the significant increase in scattering as an electron loses energy.

In this paper, we explain the importance of the effects of energy loss upon scattering in the interaction regime described above based on a unified approach derived from fundamental principles [7-9]. This model naturally links the inextricable coupling of scattering and energy loss, and will reveal several of its new and important effects.

In accordance with our approach [7-9], an integro-differential diffusion equation is solved to rigorously determine the angular and spatial distributions of the scattered electrons:

$$\frac{\partial f}{\partial s} + \mathbf{v} \cdot \nabla f = n_i \int \left[f\left(\mathbf{x}, \mathbf{v}', s\right) - f\left(\mathbf{x}, \mathbf{v}, s\right) \right] \sigma\left(\left|\mathbf{v} - \mathbf{v}'\right|\right) d\mathbf{v}', \quad (2)$$

where $f(\mathbf{x}, \mathbf{v}, s)$ is the electron distribution function; n_i the number density of fully ionized, uniform time invariant background plasma ions of charge Z, $\mathbf{x}$ the position where scattering occurs; $\sigma = \sigma_{ei} + Z\sigma_{ee}$ the total scattering cross section with σ_{ei} the Rutherford e-ion cross section [12], and σ_{ee} the Møller e-e cross section [13]. The equation is solved in cylindrical coordinates with the assumption that the scattering is azimuthally symmetric. Specifically, the angular distribution is [7-9]

$$f(\theta, E) = \frac{1}{4\pi} \sum_{\ell=0}^{\infty} (2\ell+1) P_\ell(\cos\theta) \exp\left(-\int_{E_0}^{E} \kappa_\ell\left(E'\right) \left(\frac{dE'}{ds}\right)^{-1} dE' \right),$$
(3)

where $P_\ell(\cos\theta)$ is the Legendre polynomial. In this solution, the energy loss is manifested by the plasma stopping power [14,15]

$$\frac{dE}{ds} = \frac{-2\pi r_0^2 m_0 c^2 n_i Z}{\beta^2} \left[\ln\left(\frac{\lambda_D \sqrt{\gamma-1}}{2\lambda_C} \right)^2 + 1 + \frac{1}{8}\left(\frac{\gamma-1}{\gamma} \right)^2 \right.$$
$$\left. - \left(\frac{2\gamma-1}{\gamma^2} \right) \ln 2 + \ln\left(\frac{1.123\,\beta}{\sqrt{2kT_e/m_0 c^2}} \right)^2 \right], \quad (4)$$

where $\beta = v/c$ and $\gamma = (1-\beta^2)^{-1/2}$, $r_0 = e^2/m_0 c^2$ is the classical electron radius, $\lambda_C = \hbar/m_0 c$ is electron Compton wavelength, and $\lambda_D = (kT/4\pi n_e e)^{1/2}$ is Debye length. Note that Eq. (4) is valid when $\beta \gg \alpha\ (=1/137)$, however, its classical counterpart would be accurate enough when $\beta < \alpha$, such as in the case of low-energy electron preheating inertial confinement fusion (ICF) targets. While the effects of scattering are characterized by the "macro" transport cross sections

$$\kappa_\ell(E) = n_i \int \left(\frac{d\sigma}{d\Omega} \right) [1 - P_\ell(\cos\theta)] d\Omega. \quad (5)$$

The dominant terms are $\ell=1$

$$\kappa_1(E) = 4\pi n_i \left(\frac{r_0}{\gamma\beta^2} \right)^2 \left[Z^2 \ln\Lambda^{ei} + \frac{4(\gamma+1)^2}{\left(2^{\sqrt{(\gamma+1)/2}}\right)^4} Z \ln\Lambda^{ee} \right], \quad (6)$$

which is related to the slowing-down cross section and characterizes the loss of directed velocity (momentum) in the scattering [4]; and $\ell=2$

$$\kappa_2(E) = 12\pi n_i \left(\frac{r_0}{\gamma\beta^2} \right)^2 \left[Z^2\left(\ln\Lambda^{ei} - \frac{1}{2} \right) + \frac{4(\gamma+1)^2}{\left(2^{\sqrt{(\gamma+1)/2}}\right)^4} Z\left(\ln\Lambda^{ee} - \frac{1}{2} \right) \right],$$
(7)

which is related to the deflection cross section and represents the mean-square increment in the transverse electron velocity during the scattering process [4]. It should be noted that such simple analytic versions of transport coefficients [Eqs. (6) and (7)] are only valid for $\gamma \leq 10$ [7-9], because in order to have a small angle-dominant, Rutherford-like Møller cross section, several approximations have been made. Equation (8) gives the ratio of such a simplified Møller cross section [7-9] to Rutherford cross section

$$\Re(\gamma) = Z\left(\frac{d\sigma}{d\Omega} \right)^{ee} \bigg/ \left(\frac{d\sigma}{d\Omega} \right)^{ei} \approx \frac{4(\gamma+1)^2}{\left(2^{\sqrt{(\gamma+1)/2}}\right)^4} \frac{1}{Z}. \quad (8)$$

This ratio is plotted in Fig. 2 for hydrogenic plasmas ($Z=1$), $(d\sigma/d\Omega)^{ee}$ is slightly larger (~20%) $(d\sigma/d\Omega)^{ei}$ for $\gamma < 7$ (consistent with Fig. 1), while significantly smaller for $\gamma > 10$. Figure 2 also shows that for a non-relativistic case ($\gamma = 1$), one has $(d\sigma/d\Omega)^{ee} \equiv (d\sigma/d\Omega)^{ei}$ [12]. This clearly indicates that directly applying a non-relativistic result to the cases of relativistic electron-plasmas interactions, such as fast-ignition ICF [17], results in significant inaccuracy.

The inextricable mutual couplings between energy loss and scatterings are explicitly reflected by the integrands [Eq. (3)]

$$\int_{E_0}^{E} \kappa_\ell(E') \left(\frac{dE'}{ds} \right)^{-1} dE'. \quad (9)$$

The integration is a function of electron residual energy (E). Because there is no restriction on electron energy loss, Eq. (8) is valid in the case of an arbitrary amount of even total energy loss. As shown in Fig. 3, the angular distribution converges rapidly to large angles, and its
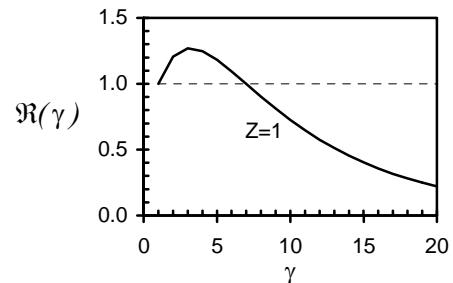
FIG. 2. The ratio of e-e scattering cross section to e-ion scattering cross section is plotted as a function of the γ.
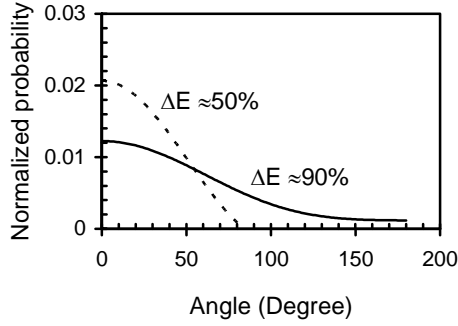
FIG. 3. The normalized angular distribution is plotted for two cases: energy loss $\Delta E \sim 50\%$ and $\Delta E \sim 90\%$.

shape is strongly dependent on the energy loss. Specifically, when energy loss is $\sim 90\%$, for example, the resulting angular distribution is characterized by a distribution with small-angle multiple scatterings plus large-angle single scatterings on the tail. In contrast, however, for energy loss $\leq 50\%$, the distribution is dominated by the small-angle scatterings.

We will see how the "thin" approximation has the result of decoupling the effects of energy loss and scattering, as discussed in Eq. (9)

$$\int_{E_0}^{E} \kappa_\ell(E')\left(\frac{dE'}{ds}\right)^{-1} dE' \approx \kappa_\ell(E)\int_{E_0}^{E}\left(\frac{dE'}{ds}\right)^{-1} dE'$$
$$= \kappa_\ell(E)S(E) \approx \kappa_\ell(E)t. \quad (10)$$

Where t is the thickness of the plasma and when it is "thin", we find that $t \approx S(E) = \int_0^S ds' = \int_{E_0}^{E}\left(dE'/ds\right)^{-1} dE'$. (The linkage of energy loss to scattering is implied by the relationship between the distance an electron transverses and energy loss, since the father an electron transverses, the more energy it loses and the more scatterings it suffers.) The approximation in Eq. (10) makes sense when ΔE is very small such that $d\sigma/d\Omega$ in Eq. (5) can be treated as independent of the energy, which in turn results in an energy-independent scattering parameter κ_ℓ which factors out the integration in Eq. (9), indicating that scattering and energy loss have been treated separately. This approximation, as discussed above and shown by Fig. 1, is of course unjustified in the case of total or even significant energy loss of energetic electrons in the plasmas which this paper is focused on.

To further illustrate the effects of energy loss on scattering, we calculate the mean-square deflection angle $<\theta^2>$ from Eq. (9). For the sake of simplicity, a small-angle scattering Fokker-Planck approximation is used by expanding the Legendre polynomial to the power of θ^2 and keeping only the first two terms [16], i.e. $P_\ell(\cos\theta) \approx 1 - 0.25\ell(\ell+1)\theta^2$. Using Eq. (3) and conducting the

integration, the first-order approximation in terms of $\int_0^S \kappa_\ell(s')ds'$ for an exponential function results in

$$\int_{E_0}^{E} \kappa_\ell(s')\left(\frac{dE'}{ds}\right)^{-1} dE' \approx \frac{1}{4}\ell(\ell+1)\langle\theta^2\rangle_{Av}, \quad (11)$$

The $\langle\theta^2\rangle$ is now ready to evaluate based on the dominant contributions from $\ell=1$ and $\ell=2$

$$\langle\theta^2\rangle \approx \sqrt{\langle\theta^2\rangle^2_{\ell=1} + \langle\theta^2\rangle^2_{\ell=2}}. \quad (12)$$

where $\quad \langle\theta^2\rangle_{\ell=1} = 2\int_{E_0}^{E}\kappa_2(E')\left(\frac{dE'}{ds}\right)^{-1} dE'.$ (13)

and

$$\langle\theta^2\rangle_{\ell=2} = \frac{2}{3}\int_{E_0}^{E}\kappa_2(E')\left(\frac{dE'}{ds}\right)^{-1} dE' \quad (14)$$

Figure 4 compares the $\langle\theta^2\rangle$ calculated from Eq. (12) and Eq. (1). As shown, a significant difference occurs when the electrons have lost more energy.

Another important result from this unified model is that the phenomenological *ad hoc* cutoffs (required to prevent mathematical divergence due to two-body Coulomb interactions) has been effectively removed because of the inclusion of energy loss in the electron scatterings. In practical applications the choosing of a suitable model for plasma screening and performing this phenomenological cutoff is a non-trivial undertaking. The *ad hoc* cutoffs directly reflect the approximations made in the theoretical formulation. Depending on the different plasma densities and temperatures, for example, b_{max} is usually determined by either Debye length, or Thomas-Fermi screening length ($\lambda_{TF} = 0.885a_0/ Z^{1/3}$) or mean inter-particle distance ($\lambda = \lambda_{Int} = n^{-1/3}$). The Debye length from an exponential screened Coulomb potential [10],
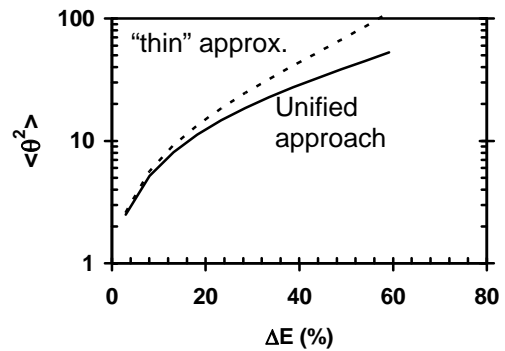

FIG. 4. Mean-square deflection angle $\langle\theta^2\rangle$ calculated from the unified approach which has taken into account the effect of energy loss on electron scattering (solid line), and compared with the conventional "thin" approximation (dashed line).

$$\phi(r) = \phi_0 e^{-r/\lambda_D}, \qquad (15)$$

describes the shielding distance at which the potential falls to its *e*-folding from its maximum. The Thomas-Fermi screening length, (a resulted derived originally from nuclear screening, with corrections for the effects of plasma temperature and density) is a reasonable approximation for ideal gas. Its accuracy requires that each Debye sphere has one single ion (for reference, in relation to the typical plasma discussed here, $\rho = 300 \text{g/cm}^3$ and $T_e = 5$ keV, with one Debye sphere having about 72 ions). Also, the mean inter-particle distance is an approximation for dense plasmas when the Debye length is even smaller than the mean inter-particle distance.

However, such a model constraint is largely relaxed due to the effective cancellation embedded in Eq. (8). For example, the electron deflection is a function of product of energy loss (dE/ds) with scatterings (κ_1),

$$\kappa_1(E)\left(\frac{dE}{ds}\right)^{-1} \propto \frac{\ln \Lambda^{ei} + \dfrac{4(\gamma+1)^2}{\left(2^{\sqrt{(\gamma+1)/2}}\right)^4} \ln \Lambda^{ee}}{\ln \Lambda}. \qquad (16)$$

The effective cancellation of the Coulomb logarithms in the numerator and denominator of Eq. (15) significantly reduces the sensitivity of the selection of plasma screening models. The physics behind such a cancellation can be understood as the deflection occurring simultaneously with the slowing down and scattering-off in the encountering plasma mediums. The result is illustrated in Fig. 5, where the normalized transport cross sections $[\kappa_1(E)(4\pi n_i)^{-1}(r_0^2/\gamma\beta^2)^{-2}]$ are plotted as a function of the energy loss [Fig. 5(a)], and differences exist for different models. As shown in Fig. 5(b) where $\kappa_1(E)(dE/ds)^{-1}$ is plotted as a function of energy loss, negligible differences will still render the effects of different models on the choice of b_{max} insignificant.

In summary, we have used an analytical model to delineate the effects of energy loss on the interactions of energetic electrons with plasmas. Our model rigorously examines the effects of energy loss upon the Coulomb interactions and reveals several new and important aspects never before realized, including the inextricable coupling of scattering and energy loss which previous calculations erroneously treated as independent of each other. The unique transparency and generality of these calculations allows for straightforward applications in the cases of partial to even total energy loss of energetic electrons: for example, the quantitative evaluation of the energy deposition of energetic electrons in various plasmas, including inertial confinement fusion plasmas.
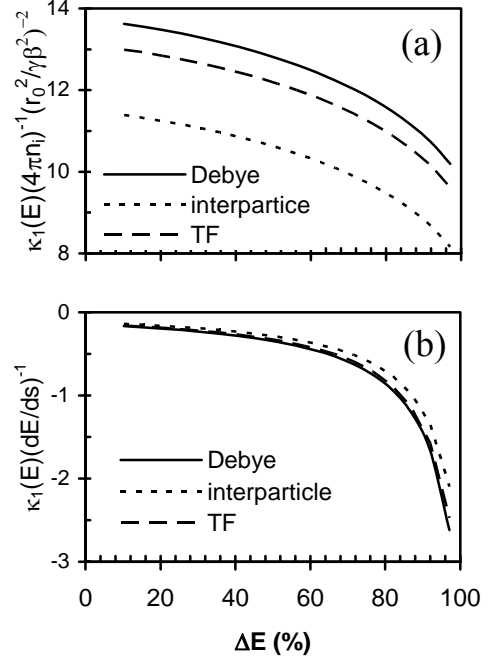
FIG. 5. Using different screening models (Debye, Thomas-Fermi, and inter-particle distance), the normalized κ_1 are plotted as a function of the electron energy in DT plasma ($\rho = 300\text{g/cm}^3$ and $T_e = 5$ keV) (a). As is shown, the difference indicates that the importance of properly choosing the screening parameters if the elastic scatterings are treated independently. However, as is seen in (b), these differences are dramatically reduced when we take the approach that energy loss and scattering coupled.

[1] G. Moliere, Z. Naturforsch. **3a**, 78 (1948).
[2] H. A. Bethe, Phys. Rev. **89**, 1256 (1953).
[3] L. Spitzer, *Physics of Fully Ionized Gases* (Interscience, New York, 1962).
[4] B. Trubnikov, *Review of Plasma Physics* (consultants Bureau, New York, 1965);
[5] C. K. Li and R. D. Petrasso, Phys. Rev. Lett. **70**, 3059 (1993).
[6] C. K. Li and R. D. Petrasso, Phys. Rev. Lett. **70**, 3063 (1993).
[7] C. K. Li and R. D. Petrasso, Phys. Rev. **E. 70**, 067401 (2004).
[8] C. K. Li and R. D. Petrasso, Phys. Rev. **E. 73**, 016402 (2006).
[9] C. K. Li and R. D. Petrasso, Phys. Plasmas **13**, 056314 (2006).
[10] J. D. Jackson, *Classical Electrodynamics* (Wiley, New York, 1975).
[11] P. C. Hemmer *et al.,* Phys. Rev. **168**, 294 (1968).
[12] R. D. Evans, *The Atomic Nucleus* (McGraw-Hill, New York, 1955).
[13] C. Møller, Ann. Physik (Leipz) **14**, 531 (1932).
[14] A. A. Solodov and R. Betti Phys. Plasmas **15** 042707 (2008).
[15] For the energy loss obtained in Ref. [7-9] we have used the classical version of the maximum impact parameter for *ad-hoc* cutoff, which may have resulted in slightly overestimated linear energy loss. In the present paper we have corrected this inaccuracy (see Eq. 4) by including quantum effects (simply replacing the Debye length λ_D by the deBroige wavelength λ_{deB} within the logarithmic term).
[16] H. W. Lewis, Phys. Rev. **78**, 526 (1950).
[17] M. Tabak *et al.,* Phys. Plasmas **1**, 1626 (1994).